How to measure the internal resistance of a battery using EIS ?

I Introduction

A battery is the association in series of a positive electrode, a separator (used here as a generic term, which includes the electrolyte) and a negative electrode. The impedance of a battery writes:

$$Z = Z_+ + Z_- + R_\Omega \quad (1)$$

where Z_+ and Z_-, are the impedance of the positive electrode and the negative electrode, respectively. R_Ω is the sum of the resistance of the separator, the current collectors and the connections. It depends on the ionic conductivity of the electrolyte contained in the separator and on the electronic conductivity of the current collectors.
During battery discharge, charge and ageing, the composition of the electrodes and the electrolyte can change and lead to a change of R_Ω. The formation or dissolution of resistive layers, parasitic reactions or the degradation of the various battery elements can also lead to a change of R_Ω, which we will refer to as internal resistance of the battery.
The aim of this note is to present different methods to measure the internal resistance using impedance measurements. It will also be explained that performing impedance measurements at several frequencies and fitting the impedance graph will reduce the incertainty in internal resistance measurement.

II Many ways to measure R_Ω

Several methods are proposed in the literature to measure the internal resistance. A dozen of methods are described in [1]. Temporal and frequential methods have been compared in EC-Lab® application notes 27, 28 and 38 [2, 3, 4]. The two most common methods are presented below.

II.1 Current interrupt

The principle of the current interrupt method, or potential-decay method, is that an ohmic contribution appears when an electrical contact is established and a non zero current is flowing. The reverse phenomenon happens when the electrical contact is switched off: the ohmic contribution disappears almost instantaneously. In EC-Lab® the sampling rate is 200 µs, which limits the temporal methods. This limitation does not apply in EIS because undersampling is used to measure frequencies that are over the sampling rate allowed by the instrument.

II.2 EIS

Measuring the internal resistance by EIS is quite an old method. We can for example mention the measurement of the separator resistance of a battery [5] or the internal resistance of lead-acid batteries [6] or NiCd batteries [7] (Fig. 1). The measurement details are not always given. Some patents describe batteries with a very small internal resistance or show a charge-discharge control device using the rate of change of internal resistance as an indicator [8, 9].

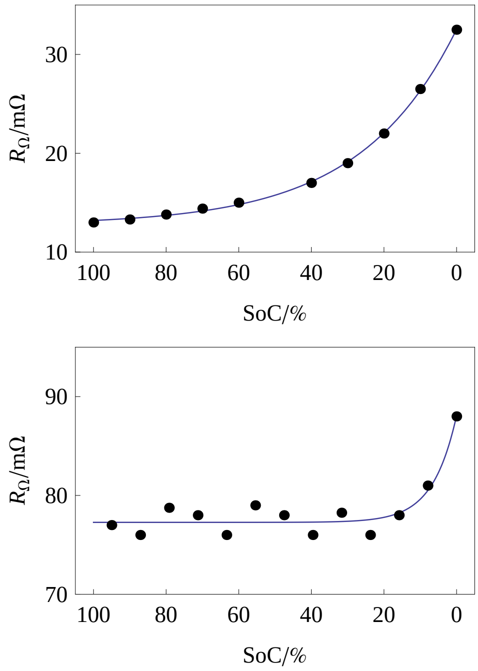

Fig. 1: Top: Change in internal resistance of a 6 V, 2.6 Ah lead-acid battery with SoC. Impedance measured at OCV. Figures taken from [6]. Bottom: internal resistance change *vs.* State of Charge (SoC) for a Mazda Ni-Cd type NCR6, 0.65 Ah battery through a 30 Ω constant load. Figure taken from [7].

III High Frequencies (HF) behaviour of the impedance of a battery

The principles of impedance measurements for batteries and their analysis are presented in the White Paper named "Studying batteries with Electrochemical Impedance Spectroscopy (EIS)". Low frequency data interpretation is given in the application note "How to interpret lower frequencies impedance in batteries ?" [10].

The behaviour of a battery separator or an electrolyte is, *a priori*, only resistive. It is only at very high frequencies that the dielectric behaviour of ionic conductors is visible [11].

An example of an impedance graph of an Li-ion battery is shown in Fig. 2. The HF limit is not resistive but is characteristic of an inductive behaviour related to the battery size, the battery connectors and the power leads. In this case, how can we measure the internal resistance ? One obvious method is to choose a particular data point.

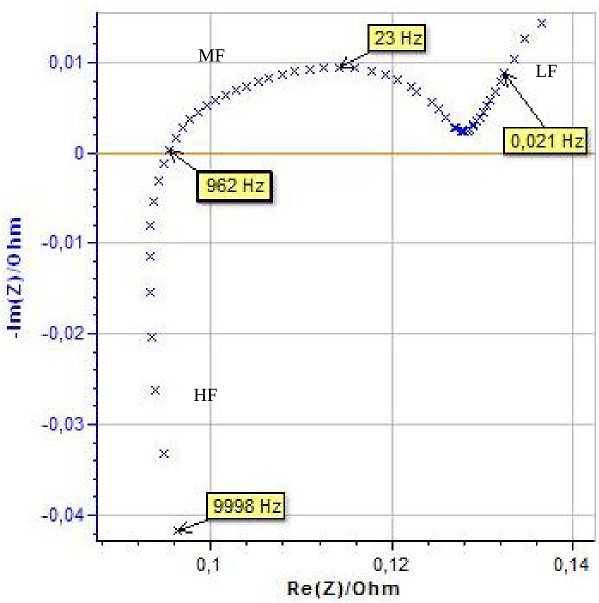

Fig. 2: Example of an impedance diagram of Li-ion battery. HF High Frequencies, MF Medium Frequencies, LF Low Frequencies.

III.1 Single point determination

Several methods of internal resistance using one impedance measurement point are used to approximate the measurement of R_Ω (Fig. 3).

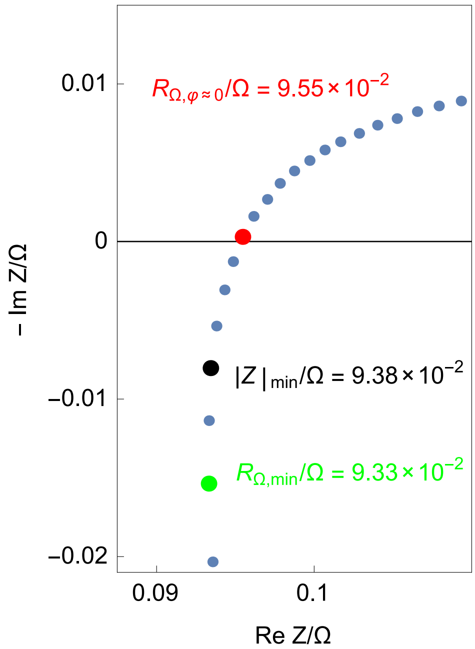

Fig. 3: Inset of the HF part of the impedance graph shown in Fig. 2. Comparison of the internal resistance measurement obtained using the impedance real part at minimal phase absolute value or zero phase (red dot), the minimal impedance module (black dot) or the minimal impedance real part (green dot).

III.1.1 Impedance real part at minimal phase absolute value $R_{\Omega,\phi=0}$

The high-frequency resistance at which the impedance diagram in the Nyquist plot intercepts the real axis (noted R_{HF}) was used to approximate the internal resistance of a lead-acid battery [12] and, more recently, of an Li-ion battery [13].
The electrochemical impedance of the system must be previously measured before performing the measurements of R_{HF}. There is no reason why for each graph there is a point at zero phase, in which case the chosen value will be the impedance real part at minimal phase absolute value (Fig. 3, red dot).

III.1.2 Minimal impedance real part $R_{\Omega,\text{min}}$

The minimal value of the impedance real part was used to approximate the internal resistance of a Li-ion battery [14]. The value corresponds to the impedance value at approximately 1 kHz and justifies the application of 1 kHz impedance measurement for characterization of aging effects.
This result is only coincidental as can be shown by the example in Fig. 2 where the 1 kHz frequency is close to the frequency of the zero phase impedance.

III.1.3 Other R_Ω measurements at a single frequency point

In the industry, single frequency measurement are often recommended, most often 1 kHz [15]. The value of minimal impedance modulus $|Z|_{\text{min}}$ could be used as an approximation of the internal resistance.

III.2 Determination by fitting an impedance graph obtained at several frequencies

In this part we will present the limitations of the single point measurement, why it cannot lead to an accurate determination of the internal resistance and why the only way to get an accurate value of the internal resistance is to perform an impedance measurement at various frequencies and perform fitting of all or part of the data.
This can be performed using EC-Lab® fitting tool Z Fit.
Another important step in the fitting process is the choice of the equivalent circuit. It can be useful to simulate impedance graphs to qualitatively validate the possible shapes of the impedance graphs of equivalent circuits

(Fig. 4). Such a simulation can be performed using Z Sim available in EC-Lab® .

III.2.1 Accounting for the battery changes

For single point measurements, the choice of the frequency is crucial. It is never certain that a correct frequency at a given state of charge or state of health will still be correct during battery operation and/or ageing.
This is the major problem when choosing a single frequency point or a single value to determine the internal resistance.

III.2.2 Accounting for the HF inductive behaviour

The influence of an inductance in series on the impedance graphs of batteries has been studied at least since 1987 [16] (Fig. 4(1)), but the HF behaviour of batteries does not always correspond to that of an inductor as is shown by the impedance graph in Fig. 2.
The impedance element:

$$Z_{\text{La}} = La\,(\mathrm{i}\,\omega)^{\alpha} \tag{2}$$

is available in Z Fit [17]. Its impedance graph is a half-line making an $\alpha\pi/2$ angle with the real axis as recalled in Fig. 4(2).
The first two cases in 4 lead to an impedance graph, whose HF limit asymptotically tends to a half-line. The HF graph is not a line anymore in the case (3) of Fig. 4, which is closer to the behaviour shown in Fig. 2. Using Z Fit or interactive files [18, 19] allows the user to simulate curves shown in Fig. 4.
The visual comparison of impedance graphs shown in Fig. 4 and in Fig. 2 lead to choose circuits R1+L2/R2 and R1+L2/R2+Q3/R3+Q4/R4+Q5 to account for the HF part of the diagram and the entire graph, respectively. Fitting results are shown in Fig. 5.

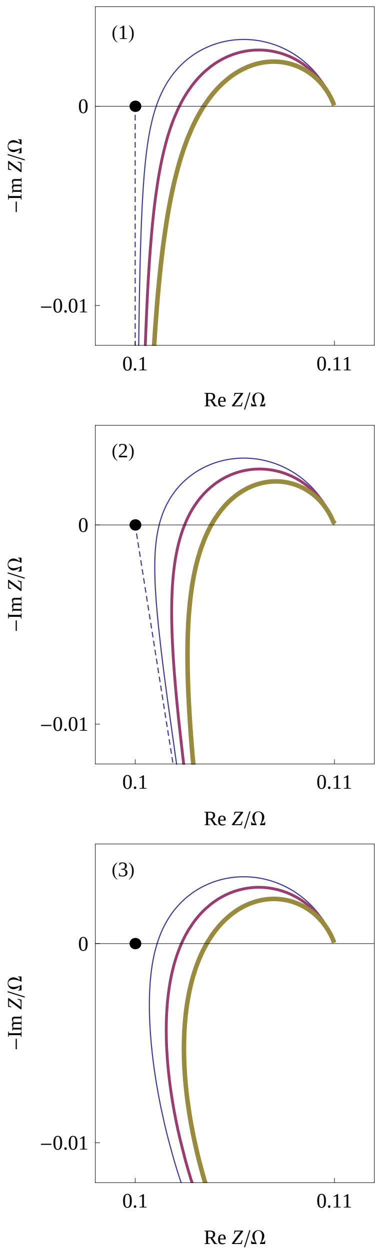

Fig. 4: Change of impedance graphs of circuits R1+L2+R3/Q3 (1), R1+La1+Q3/R3 (2) et R1+L2/R2+Q3/R3 (3) for various L1 values. The thickness of the lines increases with L1 and La1 values. The black dot corresponds to R1.

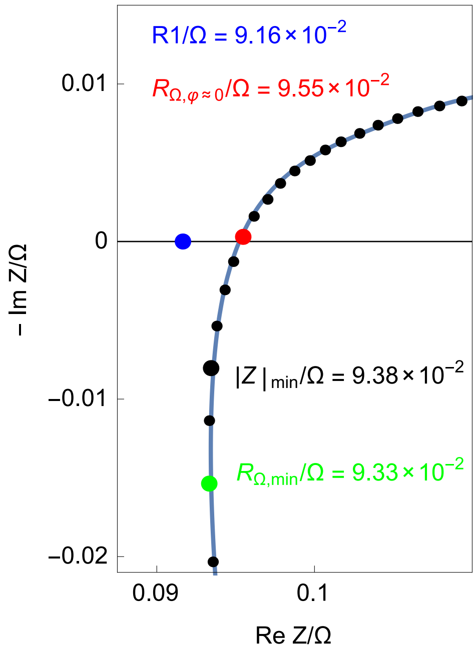

Fig. 5: HF inset of the impedance graph of Fig. 2. Line: fitting result. Comparison of the various internal resistances obtained by single point measurement methods and by fit.

The value of R1 obtained by fitting is shown in Fig. 5. Its value is lower than the values determined using a single point measurement or a single point on the impedance graph (Tab. I). For this system, the maximum difference can reach 4.26%. It could be much bigger for other systems.

Table I: Internal resistance value depending on the measurement method. $R1_{\text{fit}} = 0.0916\ \Omega$.

R	R_{mes}/Ω	$\frac{R_{\text{mes}} - R1_{\text{fit}}}{R1_{\text{fit}}}/\%$
$R_{\Omega,\phi=0}$	0.0955	4.26
$\|Z\|_{\text{min}}$	0.0938	2.40
$R_{\Omega,\text{min}}$	0.0933	1.86

IV Conclusion

Several methods can be used to measure the internal resistance of a battery using its impedance graph. It can be chosen to perform a single frequency point measurement and use the value of the real part of the impedance.
It can be chosen to perform impedance at several frequencies and to graphically choose a point on the graph for example the minimal impedance modulus or the real part of the impedance at a zero phase. This can be erroneous for two reasons:

- i) as the battery changes the correct frequency at a given battery state can be erroneous at a different state,
- ii) choosing a point on the impedance graph neglects the presence of an inductive behaviour.

Only impedance graph made at different frequencies and subsequent fitting can prevent the user from favouring a particular point on the graph, allow the user to account for the change of the battery during operation or ageing, and finally remove the effect of the inductance which can dramatically affect the resistive HF behaviour of a battery.

References

[1] H.-G. Shweiger, O. Obeidi, O. Komesker, A. Raschke, M. Schiemann, C. Zehner, M. Gehnen, M. Keller, P. Birke, Comparison of several methods for determining the internal resistance of lithium ion cells, Sensors 10 (2010) 5605 – 5625.

[2] Application note #27. Ohmic drop. I-Effect on measurements.
http://www.bio-logic.net/en/application-notes/.

[3] Application note #28. Ohmic drop. II-Introduction to Ohmic Drop measurement techniques. http://www.bio-logic.net/en/application-notes/.

[4] Application note #38. Dynamic resistance determination. A relation between AC and DC measurements? http://www.bio-logic.net/en/application-notes/.

[5] W. P. Kilroy, C. T. Moynihan, Measurement of battery separator resistances in low impedance conductivity cells by A-C bridge techniques, J. of The Electrochem. Soc. 125 (4) (1978) 520 – 522.

[6] R. Barton, P. Mitchell, Estimation of the residual capacity of maintenance-free lead acid batteries Part 1. Identification of a parameter for the prediction of state-of-charge, J. Power Sources 27 (4) (1989) 287 – 295.

[7] J.-P. Diard, B. Le Gorrec, C. Montella, EIS study of electrochemical battery discharge on constant load, J. Power Sources 70 (1998) 78 – 84.

[8] K. Kitoh, Lithium secondary battery with low internal resistance, US Patent 6,858,348 (Feb. 22 2005).

[9] T. Sakakibara, S. Sakai, Y. Nakayama, State-of-charge detector, program, method and charge-discharge control device utilizing rate of change of internal resistance, US Patent 6,987,377 (Jan. 17 2006).

[10] Application note #61. How to interpret lower frequencies impedance in batteries ? http://www.bio-logic.net/en/application-notes/.

[11] G. Barral, J.-P. Diard, B. LeGorrec, L. D. Tri, C. Montella, Impédances de cellules de conductivité. I. Détermination des plages de fréquence de mesure de la conductivité, Journal of Applied Electrochemistry 15 (6) (1985) 913 – 924.

[12] F. Huet, R. P. Nogueira, L. Torcheux, P. Lailler, Simultaneous real-time measurements of potential and high-frequency resistance of a lab cell, J. Power Sources 113 (2003) 414 – 421.

[13] I. Jiménez Gordon, S. Genies, G. Si Larbi, A. Boulineau, L. Daniel, M. Alias, Original implementation of electrochemical impedance spectroscopy (EIS) in symmetric cells: Evaluation of post-mortem protocols applied to characterize electrode materials for Li-ion batteries, J. Power Sources 307 (2016) 788 – 795.

[14] U. Troltzsch, O. Kanoun, H.-R. Trankler, Characterizing aging effects of lithium ion batteries by impedance spectroscopy, Electrochim. Acta 51 (2006) 1664 – 1672.

[15] PNGV Battery Test Manual, U.S. Department of Energy, Piscataway, USA, 2001, https://avt.inl.gov/sites/default/files/pdf/battery/pngv_manual_rev3b.pdf (last accessed in November 21, 2016).

[16] B. Savova-Stoynov, Z. B. Stoynov, Analysis of the inductance on the measured electrochemical impedance, J. Appl. Electrochem. 17 (1987) 1150 – 1158.

[17] Application note #42. ZFit : The modified inductance element La. http://www.bio-logic.net/en/application-notes/.

[18] Interactive equivalent circuit library. R1+L1+R1/C1 circuit. http://www.bio-logic.net/en/applications/eis/.

[19] Interactive equivalent circuit library. R1+L2/R2+R3/C31 circuit. http://www.bio-logic.net/en/applications/eis/.